Simulating Hemiparetic Gait in Healthy Subjects Using TPAD With a Closed-Loop Controller

Jiyeon Kang, *Member, IEEE*, Keya Ghonasgi, Conor J. Walsh, *Member, IEEE*, and Sunil K. Agrawal, *Member, IEEE*

***Abstract*— Hemiparetic gait is abnormal asymmetric walking, often observed among patients with cerebral palsy or stroke. One of the major features of asymmetric gait is excessive reliance on the healthy leg, which results in improper load shift, slow walking speed, higher metabolic cost, and weakness of the unused leg. Hence, clinically it is desirable to promote gait symmetry to improve walking. While there are no clear methods to achieve this goal, we are exploring new methods where we guide the pelvis to change the gait symmetry. This controller is designed to mimic the hands of a physical therapist holding the pelvis and guiding it to promote the usage of both legs during walking. In this paper, we show that the essence of this method can be demonstrated by promoting asymmetry in the gait of healthy subjects when walking with the device. The results showed that their kinematics and kinetics changed asymmetrically during the intervention. Subjects demonstrated asymmetric lateral ground reaction force to compensate for the lateral forces applied on the pelvis. Muscle activities increased on the targeted leg show the forced use of the leg which can be used for rehabilitation of patients with an asymmetric gait.**

***Index Terms*— Asymmetric gait pattern, pelvic guidance force, hemiparesis.**

I. Introduction

HEMIPARETIC gait is a common walking abnormality seen in patients with stroke and cerebral palsy [1]. Annually, approximately 800,000 people in the United States have a stroke [2] and 1 out of 3000 children are born with cerebral palsy [3]. Impairments in these patients are mainly on one side of their body which results in asymmetry of gait. They tend to have a longer stance time on the non-paretic limb and present asymmetric weight bearing. This is a major problem for these patients because of the following two reasons: (i) If the patient relies excessively on the non-paretic limb during walking [4], the subject will overload the joints and suffer from pain and fatigue. (ii) As paretic limb will be less used during walking, the muscles of this limb will be negatively affected due to disuse [5].

Numerous studies have tried to use locomotor adaptation to train hemiparetic patients to create symmetric gait after rehabilitation. These studies used external interventions with kinematic or dynamic constraints to reduce or augment errors of symmetry to achieve this goal. When these interventions with constraints are applied, the human nervous system adapts to the new task by recalibrating motor commands to walk in the new environment [6]. If the constraints last long enough, the adaption results in the after effects showing the possibility of changing the gait even after the intervention is removed [7].

To induce changes in the gait symmetry, researchers created kinematic constraints by adding shoe wedges or using a split-belt treadmill. Sheikh *et al.* [8] used asymmetric shoe wedges to enhance the weight bearing of stroke patients. Weight bearing while standing improved significantly after the intervention, but walking speed and spatiotemporal gait symmetry were not changed after the training. Researchers used a split-belt treadmill to increase only one belt speed to change the gait symmetry of stroke patients [9], [10]. Split-belt treadmill showed significant change in the step length symmetry but the stance time was not significantly affected compared to the conventional treadmill training [10]. Dynamic constraints on the lower limb were also reported by various research groups. For example, additional weight was added on the paretic limb to improve the symmetry of stroke patients [11]. Results of this study showed increased walking speed, step length, and range of motion, but symmetry of these parameters were not reported. As an alternative approach, Savin *et al.* [12] used perturbations prohibiting swing of one leg in hemiparetic patients walking on a treadmill. When the perturbations were removed, hemiparetic patients showed after-effects with significant changes in step-length symmetry which lasted about 20 steps after the intervention.

New mechanisms using robotic devices were developed by engineers to reduce the physical efforts of physical therapists and create more complex constraints in a repeatable and systematic manner. A research group used motorized cables

Manuscript received May 28, 2018; revised November 10, 2018 and March 15, 2019; accepted March 17, 2019. Date of publication March 27, 2019; date of current version May 9, 2019. This work was supported in part by the National Robotics Initiative Program under Grant IIS-1339666 and in part by the Cyber Physical Systems Program through the National Science Foundation under Award 1329363. *(Corresponding author: Sunil K. Agrawal.)*

J. Kang is with the Department of Mechanical Engineering, Columbia University, New York, NY 10027 USA, and also with the Department of Mechanical and Aerospace Engineering, University at Buffalo (SUNY), New York, NY 14260 USA.

K. Ghonasgi and S. K. Agrawal are with the Department of Mechanical Engineering, Columbia University, New York, NY 10027 USA (e-mail: sunil.agrawal@columbia.edu).

C. J. Walsh is with the John A. Paulson School of Engineering and Applied Sciences, Harvard University, Cambridge, MA 02138 USA, and also with the Wyss Institute for Biologically Inspired Engineering, Harvard University, Cambridge, MA 02138 USA.

Digital Object Identifier 10.1109/TNSRE.2019.2907683

to apply an assistive force on the pelvis in the medio-lateral direction which increased muscle activation of the weak leg of stroke patients [13]. This study was able to observe the forced use of one limb during the training, but a fixed amount of force based on their body weight was used for different patients. Similarly, studies with shoe wedges or weights used a constant amount of intervention for patients with different levels of asymmetry. A systematic way to quantify the proper amount of intervention could provide a customized therapy to patients and suggest a guideline of the dosage to the physical therapists based on the patient's need.

Instead of applying a defined amount of force on the body, joint or ankle trajectory based robotic intervention has also been investigated using exoskeletons like Lokomat. Lokomat moves the leg to track the desired joint angle which has shown changes in step-length symmetry of stroke patients [14]. However, the method used by Lokomat does not allow active motor control of participants during the training which is a crucial part of gait rehabilitation. To allow more active involvement during the training, assist-as-needed strategies were adopted to teach a target trajectory instead of the device moving the body segment [15].

Previously, we suggested to use multiple physical springs to apply a fixed amount of anterior-posterior force on the pelvis to teach a symmetric gait pattern to the hemiparetic patients [16]. Even though these patients generally present challenges to control the distal limb, the intervention on the pelvis could provide more flexibility to patients to account for characteristics such as spasticity, range of motion, and weakness. The suggested method applied forces on the pelvis to help them engage multiple joints and muscles to walk more symmetrically. However, the physical springs in our previous study [16] added significant inertial effect on the body and the coupling between position-force made it challenging to provide consistent force on subjects with different body sizes. To overcome these issues, we are now using actuated cables and have implemented the assist-as-needed strategy with TPAD (Tethered Pelvic Assist Device) to alter the gait symmetry [17]. This controller is able to provide different assist level at the specific phase of the gait cycle, altering the assistive force in real-time based on the patients need.

The assist-as-needed controller in TPAD mimics the hands of a therapist holding the person's pelvis to correct the abnormal pelvic motion. We hypothesized that if the pelvic motion is guided by the controller, the trajectory of the center of gravity (a point close to the pelvis center [18]) will also change to generate symmetric weight bearing. It is also expected that the patients learn the lateral ground reaction force to redirect their center of mass in the medio-lateral direction towards a more symmetric gait pattern. We hypothesized that the weakness from the learned non-use of the paretic limb will be overcome when walking with the device, similar to the previous study [19]. EMG data were observed to verify the evidence of the forced use of the targeted limb while walking with the device. The present method is mainly targeted for patients who are self-ambulatory and would like to improve their walking pattern.

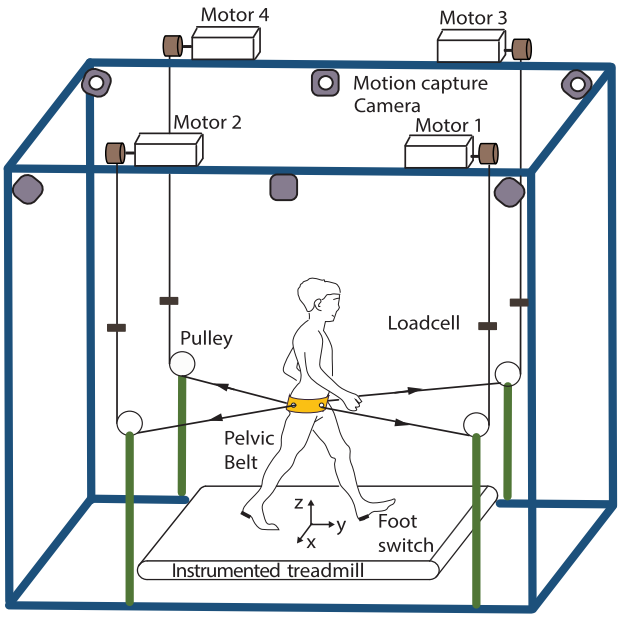

Fig. 1. System configuration with four actuated cables in the transverse plane. Cables are attached around the pelvic belt to apply forces while load cells monitored tension values in the cables. Global coordinate is defined in the middle of the instrumented treadmill with following axis: x(rightward), y(anterior), and z(vertical).

This paper consists of six different sections. Section II presents the hardware setup and salient features of the proposed force field controller. Human experiment protocol and data analysis are presented in Section III. This is followed by results in Section IV where the data of eight subjects are presented. Based on the results, Section V discusses the feasibility of this intervention with a concluding remark in Section VI.

II. Methods

A. Hardware

The cable-actuated system (TPAD) consists of several component subsystems installed around a treadmill. As shown in Fig. 1, AC single phase servo motors (Kollmorgen, Virginia) with gearboxes (Gear ratio 10:1) are mounted on a rigid frame. Cables are connected to a pelvic belt and are actuated by motors routed using pulleys. Load cells are installed in series with each cable to measure the cable tensions (Transducer Techniques, California). Four cables are attached to the pelvic belt and are arranged to lie in a horizontal plane of the pelvis to apply forces in this plane during walking. A motion capture system (Vicon, Oxford UK) is used to track the cable attachment points on the subject and determine the pelvic posture during the experiment. The control algorithm runs in real time at 200 Hz for high level controller and 1000 Hz for low level controller using Labview (National Instruments, Texas), as shown in Fig. 2(a).

B. Controller

The tensions in the cables are controlled by a 2-level control hierarchy having a high level and a low level controller.

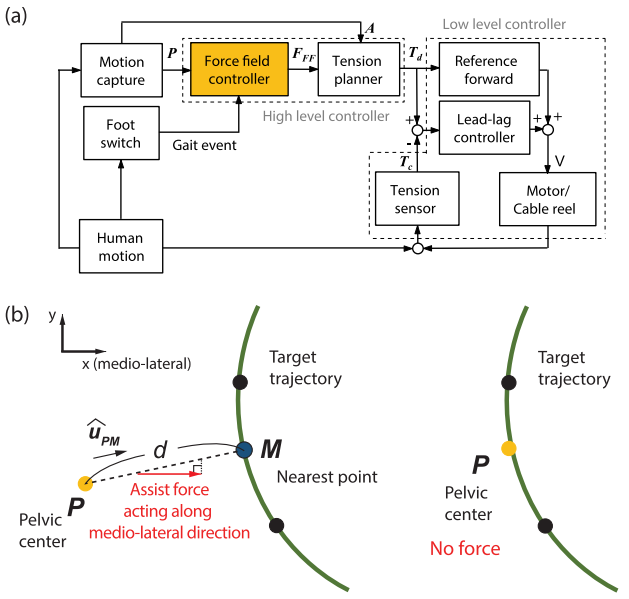

Fig. 2. (a) Control architecture of the system [17]. Force field controller that guides the pelvic center is highlighted in yellow. Motion capture system detects the posture of the pelvis *P* to compute the structure matrix *A*. Low level controller fulfills the desired tension T_d by feedforward term and lead-lag controller. (b) Schematic of the assist-as-needed controller. An assistive force is applied when the pelvic center *P* deviates from the green target trajectory. The force assistance is in the medio-lateral direction and its magnitude is proportional to the distance *d*'s projection onto the medio-lateral axis. Here, *d* is the distance between pelvic center *P* and the nearest point on the target trajectory *M*.

The role of the high level controller is to determine tensions in the individual cables to achieve a desired force and torque on the pelvis. These desired tensions in the four cables are determined by solving a quadratic programming problem with given limits on cable tensions using the structure matrix of the cable-driven parallel system [17]. The desired force is determined based on the structure of the force field controller as shown in Fig. 2(b) based on deviation of the pelvic center from a target pelvic trajectory.

1) Force Field Controller: The computation of the force field is shown in Fig. 2(b) which can be described as follows. Let P be the current position of the pelvic center (yellow dot) which is computed as the mean of the left and right iliac crest markers. M is the closest point to P on the target trajectory (blue dot). The direction of the force F_m is along the vector from P to M, denoted by the unit vector $\hat{u}_{PM}$. The magnitude of this force is defined as a function of the distance d between P and M, as shown in Eq. (1). As the distance d increases, a larger force F_m is exerted on the pelvis. The equation for the correctional force F_m is given by

$$F_m = K_m \left[1 - e^{-(d/D)^2}\right] \hat{u}_{PM}. \tag{1}$$

A damping force F_d is added to the guiding force in order to minimize oscillations. The direction of this damping force is also along the vector $\hat{u}_{PM}$ and its magnitude is proportional to the velocity of the pelvic center v. Damping force is given by

$$F_d = -K_d \left(v \cdot \hat{u}_{PM}\right) \hat{u}_{PM}. \tag{2}$$

K_m, K_d, and D in Eqs. (1–4) are constant gains. In the experiment, these constants were tuned from multiple human testing to $K_m = 45$ N, $K_d = 3$ N·s/m, and $D = 0.0125$ m. K_m was chosen to be large enough to induce changes in the pelvic displacement and K_d limits the speed of oscillation [20]. The resultant force applied on the pelvis is the total force, $F_{FF} \in \Re^3$, which is

$$F_{FF} = F_m + F_d. \tag{3}$$

From the general idea of the assist-as-needed force, this present study used only the medio-lateral component of Eq. (3).

2) Tension Planner: Tension planner computes the desired tensions from the desired force, based on the geometry of the routing cables on the belt and the frame. The tensions $T \in \Re^m$ in m cables can be obtained using the equation with a structure matrix $A \in \Re^{n \times m}$ and a wrench $W_e \in \Re^n$

$$AT = W_e, \tag{4}$$

For the case of 6-DOF wrench W_e (n =6) consisting of three-dimensional forces and moments, the matrix A is a transpose of Jacobian that relates the Cartesian space to the joint force (torque) space which can be described as:

$$A = \begin{bmatrix} \cdots & \hat{\boldsymbol{l}}_{\boldsymbol{i}} & \cdots \\ \cdots & \vec{\boldsymbol{r}}_{\boldsymbol{i}} \times \hat{\boldsymbol{l}}_{\boldsymbol{i}} & \cdots \end{bmatrix} \tag{5}$$

where $\hat{l}_i$ is the i^{th} unit cable length vector from the cable routing position on the end-effector (pelvis) B_i toward the fixed routing point P_i, and $\vec{r}_i$ is the vector from the point of application (center of pelvis) C to the i^{th} cable attachment point B_i on the end-effector. $A \in \Re^{n \times m}$ can be obtained from the cable routing positions by the motion capture system [21].

The force-moment wrench W_e was obtained from the force field controller as described in the previous section. In order to implement the force field controller, the force-moment wrench is set to be $\boldsymbol{W_e} = \left[\boldsymbol{F_x}\ \boldsymbol{F_y}\ \boldsymbol{F_z}\ \boldsymbol{M_x}\ \boldsymbol{M_y}\ \boldsymbol{M_z}\right]^{\boldsymbol{T}} = \left[\boldsymbol{F_{FF,x}}\ \boldsymbol{0}\ \boldsymbol{0}\ \boldsymbol{0}\ \boldsymbol{0}\ \boldsymbol{0}\right]^{\boldsymbol{T}}$, where $F_{FF,x}$ is the medio-lateral component of the F_{FF}. To find an optimal solution for Eq. (4) and to keep the tensions positive, an optimization problem is posed as follows:

$$\begin{aligned} &\min f,\ f = \frac{1}{2}\left[\left(T - T_p\right)^T \left(T - T_p\right)\right] \\ &\text{s.t.}\quad AT = W_e,\quad 0 < T_{max}, \end{aligned} \tag{6}$$

where T_p is the tension value at the previous time step to generate a smooth tension profile. A quadratic programming based optimization scheme with equality and inequality constraints is implemented to find the feasible solution. Ideally, to find a feasible solution for Eq. (6), a minimum number of seven cables (m=7) is needed to achieve the target wrench. This is because cables can only pull and the full six dimensional wrench can be spanned by seven cables. However, only four cables are used in this experiment by using relaxation of Eq. (6). Except the lateral force component, desired force/moment are limited to small values in the human experiment. Because this study only uses assist-as-needed force in the medio-lateral direction,

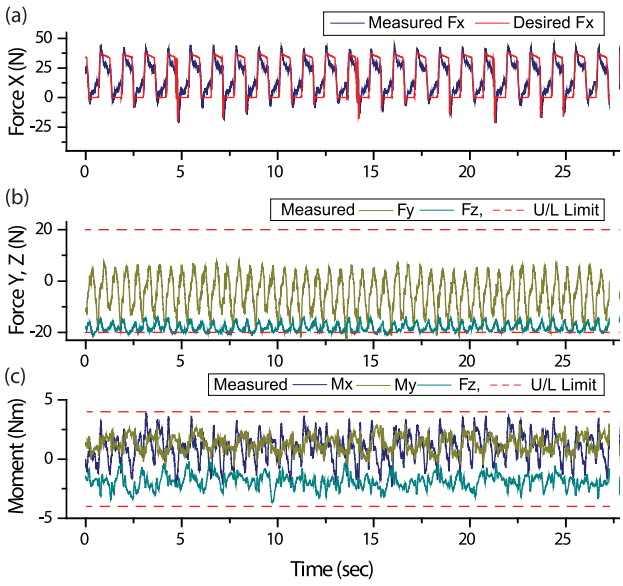

Fig. 3. (a) Desired and measured force F_X in medio-lateral direction. (b) Upper/lower limits (red dotted lines) of force F_y in anterior-posterior and F_z in vertical direction with measured force components of y and z. Upper and lower limits were set as ±4% BW. (c) Upper/lower bound (red dotted lines) of moments in three directions and measured moment components. Upper and lower bounds were set as 4 N·m.

the lateral force component of Eq. (6) is set to an equality constraint, and the other components are set to inequality constraints. For the human experiment, the moments applied on the pelvis are kept within ± 4 N·m. The constraints used in the human experiment are as below to achieve the force field force:

$$\begin{aligned} F_x &= F_{FF,x}, \\ |F_{y,z}| &\leq 4\%\ \text{BW}, \\ |M_{x,y,z}| &\leq 4\ \text{N}\cdot\text{m} \end{aligned} \tag{7}$$

The feasible workspace that satisfies Eq. (6) is verified by repeated simulations using routing points both on the fixed frame and the pelvis when a person walks on a treadmill. In case the quadratic programming does not provide a solution, the previous tension value is used as a desired tension in the low level controller.

3) Low Level Controller: The low level controller consists of feedforward and feedback terms. The feedforward term is computed from an empirical linear relationship between input voltage and tension. Feedback term is computed using a lead-lag controller. System identification was conducted prior to the controller design [22]. Using Bode plot, the lead-lag controller was set to have high gains to compensate for human low frequency motion and increase the performance of the system. Details of lead-lag controller is described in Appendix.

4) Controller Performance During Human Experiment: The performance of the controller is presented during treadmill walking in the device. Axes (x, y, z) used in Fig. 3 follow the convention in Fig. 1. Fig. 3(a) presents the measured force and desired force in the x (medio-lateral) direction. Fig. 3(b)–(c) indicate actual force/torque which are limited with lower/upper bounds. For the human experiment, y (anterior-posterior) and z (vertical) directional forces were limited to ±4% of Body Weight (BW). Torque components in all three directions were limited to ±4 N·m as well. The RMS error of the force component x (medio-lateral) is computed for one minute data as $F_x = 8.50$ N (1.55% BW). Other force or torque components that were constrained with upper/lower limits were averaged for one minute: $F_y = -3.69$ N (0.67% BW), $F_z = -18.24$ N (3.32% BW), $M_x = 0.74$ N·m, $M_y = 1.18$ N·m, and $M_z = -1.91$ N·m.

III. Human Experiment

Eight healthy adults signed a written consent form approved by the Institutional Review Board (IRB) of Columbia University before the experiment. The subject details are as follows: average height 171.4 ± 4.5 cm, average weight 61.5 ± 7.4 kg, and average age 29 ± 2.5 years. All subjects walked with their preferred treadmill speed, with an average of 0.93 ± 0.05 m/s. Markers were attached on the right & left iliac crest, sacrum, heels, first metatarsals, and the fifth metatarsals of the subject [23]. Four EMG sensors were attached to measure soleus and medial gastrocnemius for both limbs. Soleus was found at 2/3 of the line between the medial condylis of the femur to the medial malleolus. The sensor for medial gastrocnemius muscle was placed on the most prominent bulge of the muscle.

5) Protocol: The target trajectory was created from the recorded baseline data of the pelvic center of the subject with the goal to create asymmetry in the gait. Baseline data was high pass filtered with a cut off frequency of 0.4 Hz to remove slow translations on the treadmill platform. The filtered data was divided into gait cycles. This resulted in a trajectory of the pelvic center to be in the form of two wings of a butterfly as shown in Fig. 4(a). In order to create asymmetric gait of healthy subjects, the left side of medio-lateral pelvic trajectory was reduced by 40% compared to the baseline as shown in Fig. 4(a). This number was chosen to provide abnormal gait pattern of the pelvis beyond the range of standard deviation that was estimated from our previous studies with healthy human subjects [17].

The experimental protocol consisted of three sessions, as shown in Fig. 4(b). During the baseline session (BL), subjects were asked to walk for four minutes without cables and their normal walking pattern was recorded. Data was collected in the last minute of this session. The training session (T) was for twenty five minutes and the assist-as-needed force was applied on the pelvis of the subject with the TPAD. Data was collected every twelve minutes and were denoted as T1, T2, and T3. For the post-training session (PT), all cables were removed and subjects walked for another seven minutes. Data was collected at the last minute of post-training and is referred to as PT. Subjects were asked to place each foot on the corresponding split-belt of the treadmill to measure GRFs (Ground Reaction Forces) separately for right and left foot.

6) Data Analysis: All data was recorded for one minute and divided into gait cycles. A gait cycle starts with the right heel strike on the treadmill and was calculated from the foot markers and the sacrum marker [24]. The divided data was time normalized to 100% gait cycle.

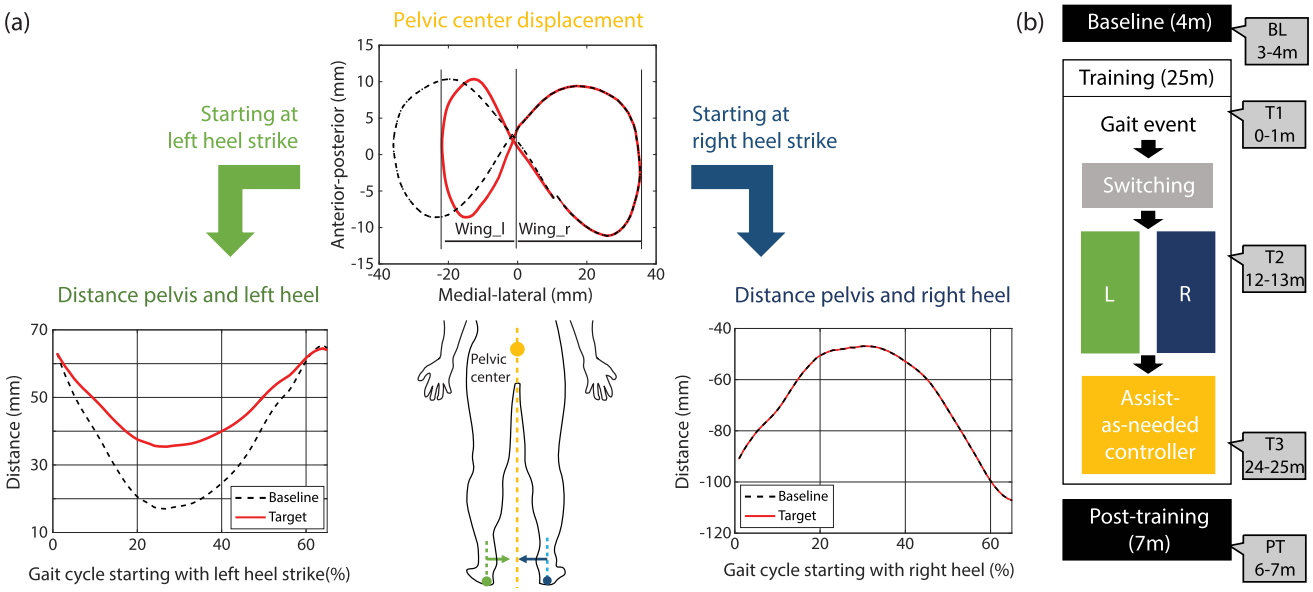

Fig. 4. (a) Design of the target pelvic trajectory to generate asymmetric weight bearing in healthy subjects. The distance between the pelvis and the heel is in medio-lateral direction. (b) Training protocol for baseline, training, and post-training sessions is presented.

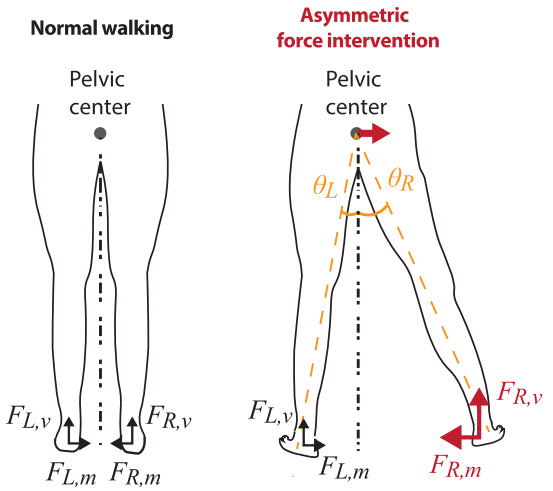

Fig. 5. Schematic of free body diagram of a subject in the back view without and with the asymmetric force intervention, where $F_{R,v}$ and $F_{L,v}$ are the vertical ground reaction forces (GRFs) while $F_{R,m}$ and $F_{L,m}$ are the medial GRFs on the right and left foot respectively. θ_R and θ_L are the lateral leg angles of the right and left foot. Under the asymmetric force intervention on the pelvic center, the parameters of $F_{R,v}$, $F_{R,m}$, and θ_R on the right side increased relative to the left side.

Kinematics, gait parameters, GRFs, and Electromyographic (EMG) signals were recorded and computed for each gait cycle, and then averaged over designated one minute. The lateral leg angles were computed from the black-dashed vertical line to the inclined yellow dashed lines as shown in Fig. 5, denoted by θ_R (right) and θ_L(left). This inclined line was created by coronal projection of the line between the sacrum and the center of the foot. The center of the foot was computed from the median of the first and fifth metatarsal markers of each foot. The parameter for lateral leg angle was defined as the averaged θ_R or θ_L over the stance period of one gait cycle.

Gait parameters were computed for each session. Step width was defined as the maximum medio-lateral distance between the right and left heel markers during the double support period. Step widths of subjects were measured at two different instances of the double stance. Right step width indicates the step width after right heel strike and left step width is measured after the left heel strike. Step length for a leg was defined as the anterior-posterior distance between the heel markers of two legs at the moment of the legs heel strike. These values were normalized by each subject's height. Stance time for each foot was computed from heel strike to toe off and normalized by the period of each gait cycle.

From force plates of the treadmill, vertical and lateral GRFs were compared between right and left foot to evaluate the symmetry of the weight bearing. It was filtered with a fourth order low pass filter with cutoff frequency 20 Hz and divided into gait cycles as well. Both EMG and GRF data were integrated and averaged over the gait cycle.

In addition, activations of those muscles which contribute actively during weight bearing were measured. Electromyographic signals were filtered with a fourth order band-pass Butterworth 40–450 Hz to remove noise and rectified. Then, a fourth order low-pass Butterworth filter (cutoff frequency: 6Hz) was used to smoothen rectified EMG envelope. For each subject, EMG data of each muscle was normalized to the maximum value recorded during the baseline session.

To understand the change in the gait symmetry, estimated parameters (P) for right and left side of limb were used to compute Symmetry Index (SI) which is defined below [25], [26]:

$$\mathrm{SI}(\%) = \frac{2(P_{right} - P_{left})}{(P_{right} + P_{left})} \times 100. \tag{8}$$

For each parameter, repeated measure ANOVA was run using data from baseline, training, and post-training sessions

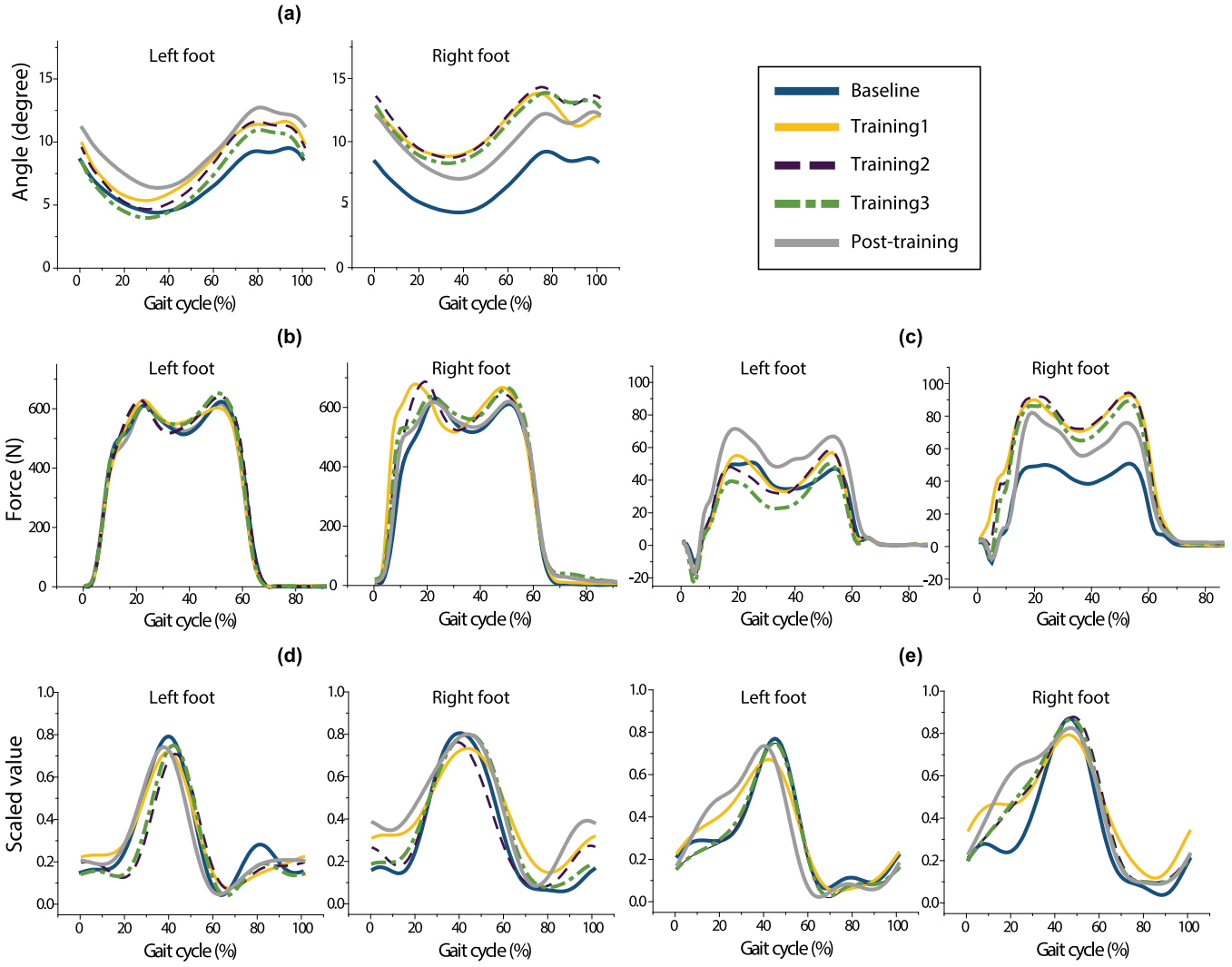

Fig. 6. Representative subject data of (a) lateral leg angles, (b) vertical ground reaction forces, (c) medial ground reaction forces (d) gastrocnemius EMG signals, and (e) soleus EMG signals for right and left foot during baseline, training, post-training sessions. Data of the left (right) foot starts with the left (right) heel strike.

($\alpha = 0.05$). In advance, Mauchly's test was conducted to check the assumption of sphericity. If sphericity was violated then Greenhouse-Geisser correction was performed for repeated measure ANOVA. For the pairwise comparison, pairwise t-test with Bonferroni-Holm correction was used for all possible combinations. All statistical analysis was conducted using SPSS (IBM, New York).

IV. Results

Data of one representative subject and the group is shown in Figs. 6–7 for kinematics, ground reaction forces, and EMG. Repeated measures ANOVA (rANOVA) results are presented with F and corrected p values. Gait parameters, stance phase, step width, and step length are tabulated in Table I. For each variable, rANOVA was run separately three times on Symmetry Index (SI), right leg, and left leg. This was to evaluate changes in variables of individual leg as well as the right/left ratio. The stance phase of the group became asymmetrical during training, where $F(4, 28) = 5.241$ and $p = 0.003$. It shows a strong asymmetry in the initial training session (T1) and then subjects adapted to the guidance force and reduced asymmetry in the later part of training.

Symmetry index of the step width is computed by right and left step widths using Eq. (8), but significant changes weren't found. When each step widths were evaluated separately with rANOVA through different training sessions, both right and left step width showed significant change. Both right and left step width increased during T1 when the force intervention started. During T2 and T3, their increment reduced when subjects adapted to the guidance force. The step width after right heel strike ($F(1.608, 11.259) = 8.02$, $p = 0.009$) presented significant pairs: BL-T1 ($p<0.001$), BL-T2 ($p=0.010$), and BL-T3($p=0.021$). Also, the step width after left heel strike ($F(1.602, 11.318) = 8.945$, $p = 0.006$) has significant pairs BL-T1 ($p<0.001$), BL-T2 ($p=0.009$), and BL-T3 ($p=0.011$). In short, subjects increased both the step width after right and left heel strike during the training, but there wasn't any difference between the right and left step width. After

TABLE I
GAIT PARAMETERS OF STANCE PHASE, STEP WIDTH, AND STEP LENGTH. RANOVA WAS RUN SEPARATELY FOR SYMMETRY INDEX, RIGHT LEG, AND LEFT LEG.

Parameters		BL	T1	T2	T3	PT
Stance (%)	Sym. Index*	-0.174 ±0.478	2.694 ±1.292	1.360 ±0.706	0.246 ±0.510	0.332 ±0.762
	Right	66.359 ±0.260	66.628 ±0.655	66.226 ±0.348	65.958 ±0.302	65.503 ±0.762
	Left	66.474 ±0.231	64.839 ±0.279	65.329 ±0.281	65.797 ±0.315	65.306 ±0.968
Scaled step width	Sym. Index	1.06 ±0.88	-2.354 ±0.658	-1.0202 ±1.556	-1.488 ±1.156	2.75 ±2.132
	Right*	0.135 ±0.002	0.185 ±0.005	0.172 ±0.007	0.172 ±0.008	0.156 ±0.014
	Left*	0.133 ±0.002	0.189 ±0.005	0.176 ±0.009	0.175 ±0.009	0.153 ±0.015
Scaled step length	Sym. Index	-1.574 ±0.878	-6.752 ±2.826	-8.418 ±3.354	-3.39 ±1.894	-4.944 ±4.246
	Right	0.309 ±0.006	0.278 ±0.004	0.270 ±0.013	0.295 ±0.005	0.292 ±0.014
	Left	0.313 ±0.005	0.298 ±0.008	0.292 ±0.009	0.305 ±0.007	0.305 ±0.007

* indicates significant change with $\alpha = 0.05$.

the force was removed from the pelvis, subjects still had higher step width than their baseline, but no significance was found.

Similarly, the step length was measured for right and left step separately. Symmetry index using Eq. (8) was also computed using the right and left step lengths. Symmetry index of step length showed asymmetric trend during the training which was reduced over time. Due to large variation among subjects, significance was not found. Both step lengths of each right and left leg showed decreasing trend, but no significance was reported.

Lateral angle in Fig. 6(a) shows that both left and right leg angles increased after onset of force compared to the baseline (See also Fig. 11(a)). For the group data, symmetry index of lateral leg angle increased after the initiation of force intervention and plateaued at T2. The training effect went away after the tethers of the device were removed from the pelvis. Symmetry index of group showed significant change with $F(4, 28) = 19.287$ and $p < 0.001$. Pairwise comparison reported significance in BL-T3 (p=0.002), BL-T4 (p=0.001), T3-PT (p=0.002), and T4-PT (p=0.002) pairs.

GRFs were evaluated for vertical and lateral directions as shown in Fig. 6(b)–(c) and Fig. 7(b)–(c) present the lateral and vertical GRF of subjects. The lateral GRF demonstrated similar trend as the lateral leg angle. Lateral GRF increased after the intervention, but there wasn't any retention observed during the post-training session of the group data ($F(4, 20) = 110.761$ and $p < 0.001$). All significant pairs during the training are marked in Fig. 7(b): T1-T3 (p=0.020), T1-T2 (p=0.024), BL-T1 (p=0.001), BL-T2 (p=0.001), T1-PT (p<0.001), T2-PT (p<0.001), T3-PT (p<0.001), and BL-T3 (p<0.001). Vertical GRF showed a different trend during the training. Instead of increasing and getting plateaued, the increment of vertical GRF decreased over time during the training session ($F(4, 28) = 5.901$ and $p = 0.001$). The significant pair of vertical GRF was only BL-T1 (p=0.01549).

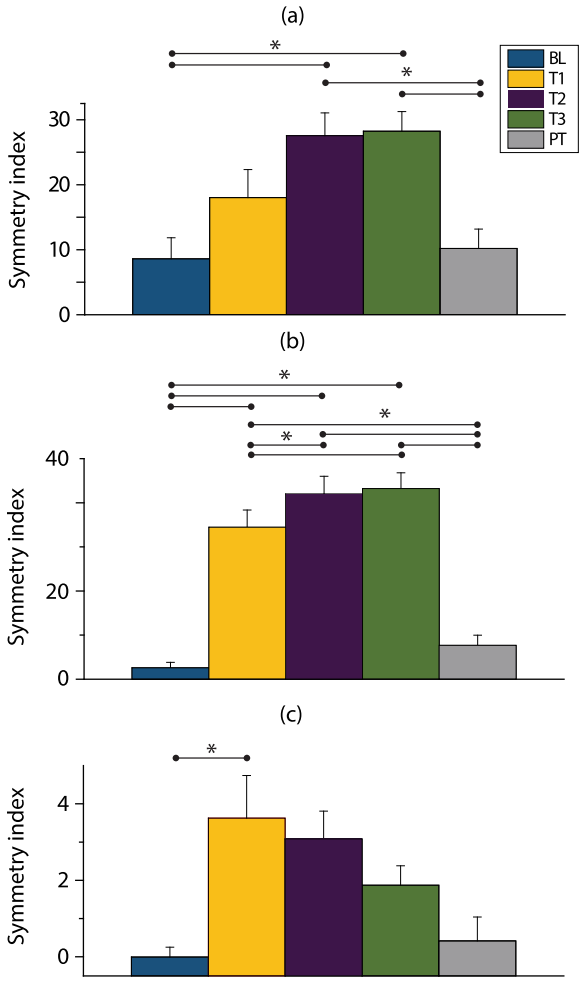

Fig. 7. Asymmetry is estimated using symmetry index for (a) lateral leg angle with respect to the vertical line, (b) medial ground reaction force (n=6), and (c) vertical ground reaction force with $p < 0.05$. Positive symmetry index indicates that right leg's value is higher than the left one.

Results of leg angles and GRFs show that subjects chose compensatory methods to cancel the extra force applied on the pelvis and its corresponding torque. The diagram in Fig. 5 shows the major component of guidance force acting on the subject during normal walking and TPAD intervention. TPAD applies a force on the pelvis directed along the right of the subject due to the nature of the target trajectory shown in Fig. 4(a). The force starts to act at the left heel strike and prohibits the progression of Center of Mass (CoM) to the left by applying a right directional force. While the subject resisted against the force that pulled the body to the right, the medial GRF of right leg $F_{R,m}$ increased. To prevent rotating towards right side, subjects chose two different strategies to apply counter torque. They increased the vertical GRF to resist the moment created by the extra lateral force from TPAD. Also, subjects increased the moment arm of the right leg. The right leg made a wider step than the left leg to increase the counter clockwise moment to keep stability while walking.

Fig. 8(a)–(b) present the EMG signals of the gastrocnemius and soleus muscles. These two muscles were observed during the stance of the gait when supporting the body [27]. From the

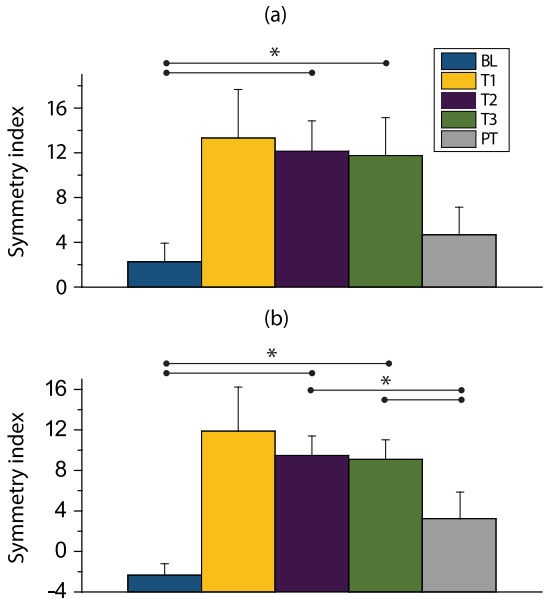

Fig. 8. (a) Gastrocnemius and (b) soleus EMG signals demonstrate significant increases in the asymmetry that is computed by the difference between the right and left leg's EMG value.

experiment design, the symmetry index is expected to increase which means the subject is bearing more weight on the right foot in comparison to the left foot. First, the significant increase in the asymmetric EMG signal of the gastrocnemius is observed during the training as in Fig. 8(a): $F(4, 28) = 6.215$ and $p = 0.001$. Asymmetry of gastrocnemius muscle increased immediately after initiation of the training and lasted until later part of the training. As significant pairs, BL-T2 (p=0.002) and BL-T3 (p=0.007) are reported. However, activation of gastrocemius decreased during the post-training when the device was removed from the pelvis. Similarly, the soleus muscles are also activated asymmetrically during the training session, where $F(4, 28) = 6.862$ and $p = 0.001$. Pairwise t-test reported significant pairs of soleus for BL-T2 (p=0.002), BL-T3 (p=0.019), T2-PT (p=0.021), and T3-PT (p=0.023).

EMG patterns were observed for gastrocnemius and soleus muscles which are responsible for bearing the weight during the stance. Increased asymmetry in soleus and gastrocnemius (plantar flexor) muscles were observed with the increased asymmetry of vertical GRF. But, the later part of training demonstrated different trend between vertical GRF and plantar flexor muscles. Increase of asymmetry in vertical GRF decreased in the latter part of the training, but symmetry index of plantar flexor muscles had a similar level until the end of the training. This could be presumably explained by additional role of plantar flexor muscles. These muscles accelerate the center of mass generally in the vertical and anterior directions, but they also generate partial mediolateral ground reaction force to accelerate the CoM laterally.

V. Discussion

A new method was investigated with a virtual hand that guides the pelvis to promote gait symmetry. While testing with healthy subjects, various symmetry indices were used to assess the possible benefits for the hemiparetic subjects and the evidence of the forced use of the targeted limb. Additionally, we carefully investigated the biomechanics of the participants to understand the effect of force during treadmill walking. When subjects walked with the virtual hand on the pelvis, subjects presented different gait patterns.

Healthy subjects showed increased asymmetry in their muscle activation during stance in response to the forced use of one leg. Increasing soleus muscle and medial gastrocnemius can be beneficial to subjects with hemiparesis for two different reasons. Soleus muscle is responsible for the weight bearing during the stance which can support the trunk and promote a stable stance of the limb [28]. Gastrocnemius muscle also activates during the stance phase, but it plays a more crucial role for the leg during swing. Gastrocnemius muscle pushes off the limb against the ground during the stance to flex the knee and initiate the swing of that leg. Increased gastrocnemius activation can generate better propulsion and foot clearance of the paretic leg which is typically challenging in patients with hemiparesis. It has been also shown in our previous study that the patients are observed to improve the swing of the leg when the paretic limb is forced to use for longer time [23]. As a result of walking with the virtual hand, participants increased asymmetry in the lateral ground reaction force to adapt in a new environment with force constraints. They increased the lateral ground reaction force until the end of the training to compensate for the lateral force on the pelvis. Patients can use this learned lateral ground reaction force to redirect their center of mass in the medio-lateral direction towards a more symmetric gait pattern. Lateral motion of the center of mass can create a significant impact on the gait, as the lateral movement of center of mass shifts the weight to one leg and enables swing of the other leg.

This training targeted forced stance of the leg, but the percentage of the stance within the gait cycle was not significantly increased. Similar results were reported in the previous study with lateral pelvic pull [13]. This study also reported increased muscle activation, but the stance symmetry did not change. Changes in the stance time was only reported in the interventions that included temporal constraints like split-belt treadmill [9]. From this perspective, we conclude that the stance time was not changed due to the nature of the intervention. In addition, We investigated the vertical ground reaction force to estimate approximated weight bearing when the participant walked on the treadmill. The asymmetry in vertical ground reaction force was only presented in the initial part of the training and faded out as the subject adapted to the intervention by increasing the step width. Previous studies with asymmetric shoe wedges showed longer and consistent changes in the weight bearing, but this data was estimated when the subject was standing stationary which made it difficult for fair comparison to the present study [8].

Despite the present demonstration of simulating asymmetric gait pattern of healthy subjects, further studies may still be required to translate this novel training to patient groups. Earlier literature has argued that healthy subjects and patients with impairments may respond differently as the biomechanical characteristics and capabilities of patients are different

from healthy subjects [29]. Healthy subjects walked with an asymmetric gait that they weren't used to which required extra effort. Retention in patients might differ from healthy subjects, as their gait will be guided to be more symmetric than their original asymmetric gait. In addition, we will include stationary standing to measure the weight bearing for equivalent comparison to the existent literature.

Our future study will add an asymmetrical vertical force to the lateral pull to enhance asymmetric weight bearing. From this study, we found that subjects generated a mediolateral force to cancel out the external force/torque generated from TPAD and increased asymmetry in their gait. If a direct vertical force from TPAD is applied on the impaired leg of the subject, they will increase their vertical ground reaction force of that leg to cancel out the extra force from TPAD. Further studies may still be required with patient groups, but we envision that this novel training paradigm can change symmetry in weight bearing of hemiparetic patients.

VI. Conclusion

The present study with healthy subjects shows the feasibility of the forced use of leg to affect the gait symmetry in muscle activation, ground reaction force, and kinematics during the training. This present controller suggests a unique method that provides a guidance force that is computed by the individual pelvic motion to promote the forced-use of the targeted leg. We envision that the suggested training would further help the patients with hemiparesis to have stronger paretic limb and enhance the symmetry of the gait pattern.

Appendix

7) Low Level Controller: This part reports system modeling and controller design of the cable actuated system that was used during the human experiment. System identification was conducted for one actuation unit that consists of one AC motor, one cable winch, one tension sensor, and a real time controller. Experiment was conducted by fixing the end of the cable on a rigid frame. Input command was sent to the motor drive with different frequency that ranges between 10^{-1}–10^{2} Hz. The data collected from each frequency was used to constitute a bode plot and then system identification was conducted using the subspace identification technique [30] with Matlab built-in function `n4sid`. Fig. 9 presents the bode plot with actual data points and the fitted model in solid green line. From the identification, transfer function matrix $G(s)$ between the cable tension value and the actuator input is defined as below:

$$G(s) = \frac{-532.5s^2 + 9.928^4 s + 9.788 \times 10^5}{s^3 + 105.2s^2 + 7754s + 4.881 \times 10^4} \quad (9)$$

Phase delay that is observed in low frequency region is presumably due to the friction, deadband, and nonlinear behavior of the cable actuated system.

The goal of this lead-lag controller in Fig. 10 is to increase the gain of the low frequency inputs for compensating human motion that is delivered to the system while keeping the system stable. The crossover frequency was set to be $\omega_c = 60$ Hz and desired phase margin was $\phi_m = 60°$. To achieve the desired phase margin, extra phase lead was added to make the system stable. The values chosen for the lead-lag controller were $\omega_{p,ld} = 15.32$, $\omega_{z,ld} = 26.11$, and $\omega_{z,lg} = 10$. In addition,

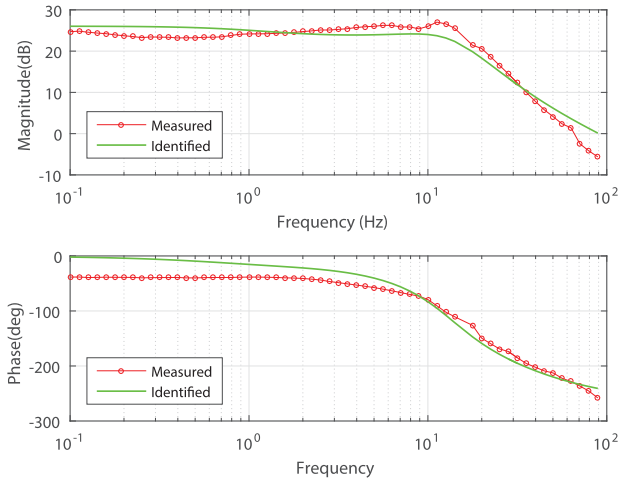

Fig. 9. System identification of one cable actuation unit. The mathematical model of this plant was estimated by using matlab function `n4sid`.

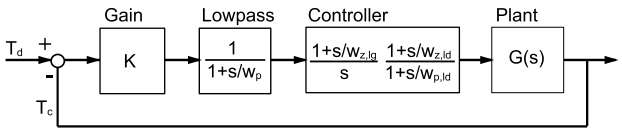

Fig. 10. Control diagram of lead-lag controller for each control unit. T_d is computed from the tension planner in high level controller and T_c is measured from the tension sensor that is connected to the cable in series.

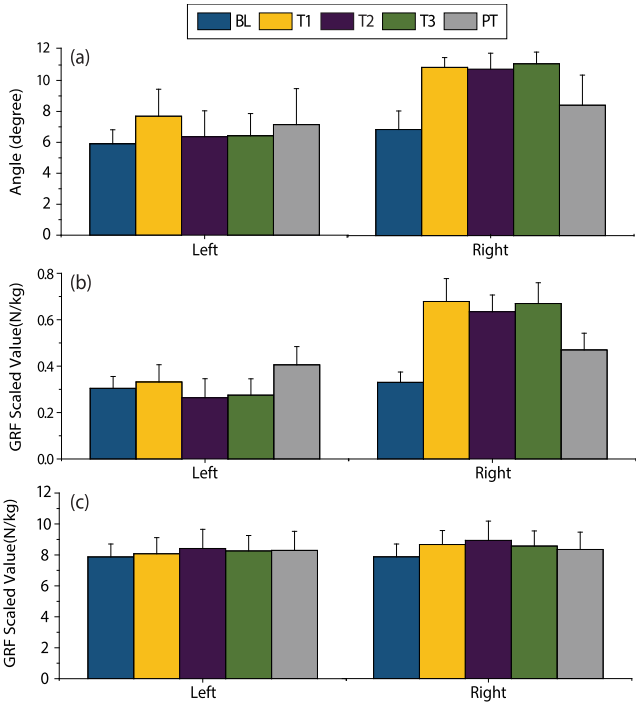

Fig. 11. Right and left leg data with average and standard deviation: (a) lateral leg angle, (b) medial ground reaction force, and (c) vertical ground reaction force.

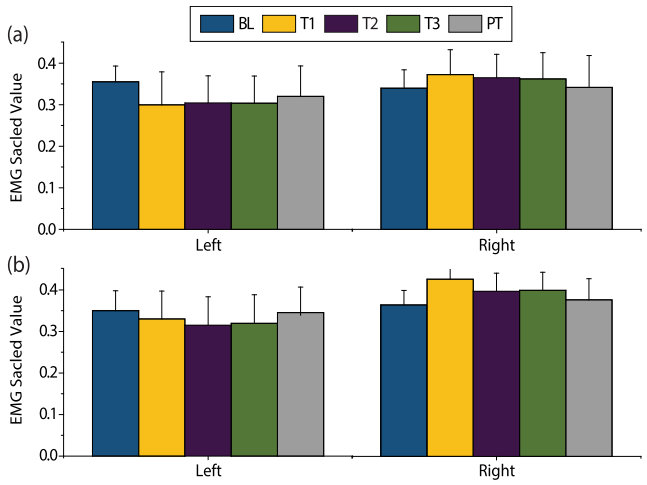

Fig. 12. Right and left leg data with average and standard deviation: (a) gastrocnemius EMG and (b) soleus EMG.

lowpass filter was added with a pole ($w_p = 10$) in order to remove high frequency noise to the system while applying high value of gain ($k = 200$).

8) Parameter Plots for Right and Left Legs: Parameters used to compute the symmetry indices are presented for each right and left leg. Lateral angles and ground reaction forces are shown in Fig. 11. Gastrocnemius and soleus data of left and right legs are demonstrated in Fig. 12.

REFERENCES

[1] K.-H. Mauritz, "Gait training in hemiplegia," *Eur. J. Neurol.*, vol. 9, no. s1, pp. 23–29, 2002.

[2] A. S. Go *et al.*, "Executive summary: Heart disease and stroke statistics–2013 update: A report from the American Heart Association," *Circulation*, vol. 127, no. 1, pp. 143–152, 2013.

[3] S. Winter, A. Autry, C. Boyle, and M. Yeargin-Allsopp, "Trends in the prevalence of cerebral palsy in a population-based study," *Pediatrics*, vol. 110, no. 6, pp. 1220–1225, 2002.

[4] S. G. Kirker, D. S. Simpson, J. R. Jenner, and A. M. Wing, "Stepping before standing: Hip muscle function in stepping and standing balance after stroke," *J. Neurol. Neurosurg. Psychiatry*, vol. 68, no. 4, pp. 458–464, 2000.

[5] K. K. Patterson *et al.*, "Gait asymmetry in community-ambulating stroke survivors," *Arch. Phys. Med. Rehabil.*, vol. 89, no. 2, pp. 304–310, Feb. 2008.

[6] A. J. Bastian, "Understanding sensorimotor adaptation and learning for rehabilitation," *Current Opinion Neurol.*, vol. 21, no. 6, p. 628, 2008.

[7] T. Lam, M. Anderschitz, and V. Dietz, "Contribution of feedback and feedforward strategies to locomotor adaptations," *J. Neurophysiol.*, vol. 95, no. 2, pp. 766–773, Feb. 2006.

[8] M. Sheikh, M. R. Azarpazhooh, and H. A. Hosseini, "Randomized comparison trial of gait training with and without compelled weight-shift therapy in individuals with chronic stroke," *Clin. Rehabil.*, vol. 30, no. 11, pp. 1088–1096, 2016.

[9] D. S. Reisman, R. Wityk, K. Silver, and A. J. Bastian, "Split-belt treadmill adaptation transfers to overground walking in persons poststroke," *Neurorehabil. Neural Repair*, vol. 23, no. 7, pp. 735–744, 2009.

[10] M. D. Lewek, C. H. Braun, C. Wutzke, and C. Giuliani, "The role of movement errors in modifying spatiotemporal gait asymmetry post stroke: A randomized controlled trial," *Clin. Rehabil.*, vol. 32, no. 2, pp. 161–172, 2018.

[11] J. Regnaux, D. Pradon, N. Roche, J. Robertson, B. Bussel, and B. Dobkin, "Effects of loading the unaffected limb for one session of locomotor training on laboratory measures of gait in stroke," *Clin. Biomech.*, vol. 23, no. 6, pp. 762–768, 2008.

[12] D. N. Savin, S. M. Morton, and J. Whitall, "Generalization of improved step length symmetry from treadmill to overground walking in persons with stroke and hemiparesis," *Clin. Neurophysiol.*, vol. 125, no. 5, pp. 1012–1020, 2014.

[13] C.-J. Hsu, J. Kim, R. Tang, E. J. Roth, W. Z. Rymer, and M. Wu, "Applying a pelvic corrective force induces forced use of the paretic leg and improves paretic leg EMG activities of individuals post-stroke during treadmill walking," *Clin. Neurophysiol.*, vol. 128, no. 10, pp. 1915–1922, 2017.

[14] K. P. Westlake and C. Patten, "Pilot study of lokomat versus manual-assisted treadmill training for locomotor recovery post-stroke," *J. Neuroeng. Rehabil.*, vol. 6, no. 1, p. 18, 2009.

[15] S. K. Banala, S. K. Agrawal, S. H. Kim, and J. P. Scholz, "Novel gait adaptation and neuromotor training results using an active leg exoskeleton," *IEEE/ASME Trans. Mechatronics*, vol. 15, no. 2, pp. 216–225, Apr. 2010.

[16] V. Vashista, D. S. Reisman, and S. K. Agrawal, "Asymmetric adaptation in human walking using the tethered pelvic assist device (TPAD)," in *Proc. IEEE Int. Conf. Rehabil. Robot. (ICORR)*, Jun. 2013, pp. 1–5.

[17] J. Kang, V. Vashista, and S. K. Agrawal, "On the adaptation of pelvic motion by applying 3-dimensional guidance forces using TPAD," *IEEE Trans. Neural Syst. Rehabil. Eng.*, vol. 25, no. 9, pp. 1558–1567, Sep. 2017.

[18] M. W. Whittle, "Three-dimensional motion of the center of gravity of the body during walking," *Hum. Movement Sci.*, vol. 16, no. 2, pp. 347–355, 1997.

[19] C.-J. Hsu, J. Kim, E. J. Roth, W. Z. Rymer, and M. Wu, "Forced use of the paretic leg induced by a constraint force applied to the nonparetic leg in individuals poststroke during walking," *Neurorehabil. Neural Repair*, vol. 31, no. 12, pp. 1042–1052, 2017.

[20] J. Kang, V. Vashista, and S. K. Agrawal, "A novel assist-as-needed control method to guide pelvic trajectory for gait rehabilitation," in *Proc. IEEE Int. Conf. Rehabil. Robot. (ICORR)*, Aug. 2015, pp. 630–635.

[21] V. Vashista, X. Jin, and S. K. Agrawal, "Active tethered pelvic assist device (A-TPAD) to study force adaptation in human walking," in *Proc. IEEE Int. Conf. Robot. Autom. (ICRA)*, May 2014, pp. 718–723.

[22] K. Ogata and Y. Yang, *Modern Control Engineering*. Upper Saddle River, NJ, USA: Prentice-Hall, 1970.

[23] J. Kang, D. Martelli, V. Vashista, I. Martinez-Hernandez, H. Kim, and S. K. Agrawal, "Robot-driven downward pelvic pull to improve crouch gait in children with cerebral palsy," *Sci. Robot.*, vol. 2, no. 8, p. eaan2634, 2017.

[24] J. A. Zeni, J. G. Richards, and J. S. Higginson, "Two simple methods for determining gait events during treadmill and overground walking using kinematic data," *Gait Posture*, vol. 27, no. 4, pp. 710–714, 2008.

[25] C. M. Kim and J. J. Eng, "Symmetry in vertical ground reaction force is accompanied by symmetry in temporal but not distance variables of gait in persons with stroke," *Gait Posture*, vol. 18, no. 1, pp. 23–28, 2003.

[26] G. Chen, C. Patten, D. H. Kothari, and F. E. Zajac, "Gait deviations associated with post-stroke hemiparesis: Improvement during treadmill walking using weight support, speed, support stiffness, and handrail hold," *Gait Posture*, vol. 22, no. 1, pp. 57–62, 2005.

[27] J. Perry and B. Schoneberger, *Gait Analysis: Normal and Pathological Function*. Thorofare, NJ, USA: Slack, 1992.

[28] D. A. Winter, *The Biomechanics and Motor Control of Human Gait: Normal, Elderly and Pathological*. Hoboken, NJ, USA: Wiley, 1991.

[29] J. C. Dean and S. A. Kautz, "Foot placement control and gait instability among people with stroke," *J. Rehabil. Res. Dev.*, vol. 52, no. 5, p. 577, 2015.

[30] T. McKelvey, H. Akcay, and L. Ljung, "Subspace-based multivariable system identification from frequency response data," *IEEE Trans. Autom. Control*, vol. 41, no. 7, pp. 960–979, Jul. 1996.